

DIQ-H: Evaluating Hallucination Persistence in VLMs Under Temporal Visual Degradation

Zexin Lin^{1,3,*}, Hawen Wan^{1,3,*}, Yebin Zhong^{1,3}, and Xiaoqiang Ji^{1,2,3,†}

Abstract—Vision-Language Models (VLMs) deployed in safety-critical applications like autonomous driving must handle continuous visual streams under imperfect conditions. However, existing benchmarks focus on static, high-quality images, ignoring temporal degradation and error propagation—critical failure modes where transient visual corruption induces hallucinations that persist across subsequent frames. We introduce DIQ-H, the first benchmark evaluating VLM robustness under dynamic visual degradation in temporal sequences. DIQ-H applies physics-based corruptions (motion blur, sensor noise, compression artifacts) and measures hallucination persistence, error recovery, and temporal consistency through multi-turn Q&A tasks. To enable scalable annotation, we propose Uncertainty-Guided Iterative Refinement (UIR), which generates reliable pseudo-ground-truth via lightweight VLMs with uncertainty filtering, achieving 15.3% accuracy improvement. Experiments on 16 state-of-the-art VLMs reveal significant robustness gaps: even top models like GPT-4o show only 78.5% recovery rate, while open-source models struggle with temporal consistency (<60%). DIQ-H provides a comprehensive platform for evaluating VLM reliability in real-world deployments.

Index Terms—Large Vision-Language Models, Error Propagation, Automated Annotation, Multimodal Benchmarking, Robustness Evaluation

I. INTRODUCTION

Vision-Language Models (VLMs) are increasingly deployed in safety-critical applications such as autonomous driving and robotic manipulation, where they must interpret continuous visual streams under imperfect conditions. A fundamental challenge is *hallucination*—the tendency to fabricate non-existent objects or attributes—which becomes particularly dangerous when errors compound over time in sequential reasoning tasks.

Limitations of Existing Benchmarks. Current evaluation paradigms suffer from three critical gaps: (1) *Static focus*: Benchmarks like LLaVA-Bench [1] and MME [2] assess only single-frame understanding; (2) *Temporal blindness*: Hallucination benchmarks (POPE [3], AMBER [4]) evaluate isolated responses without modeling error propagation; (3) *Idealized inputs*: Video benchmarks (ConBench [5]) assume pristine quality, ignoring real-world degradation from motion blur, sensor noise, and compression artifacts. These limitations obscure a critical failure mode: *cognitive inertia*, where hallucinations

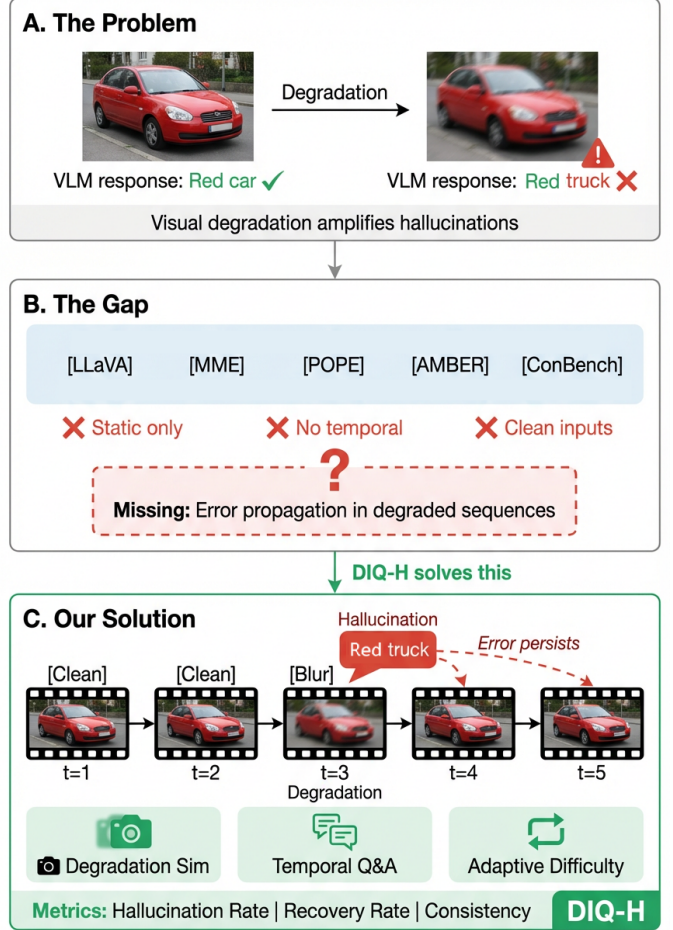


Fig. 1. Overview of motivation and approach. (a) VLMs hallucinate under degradation. (b) Existing benchmarks ignore temporal error propagation. (c) DIQ-H evaluates hallucination persistence and recovery under dynamic degradation.

induced by transient degradation persist even after visual quality recovers.

Our Approach. We introduce DIQ-H (**D**egraded **I**mage **Q**uality leading to **H**allucinations), the first benchmark to evaluate VLMs under dynamic visual degradation in temporal sequences. DIQ-H addresses the above gaps through: (1) *Physics-based degradation simulation* applying realistic motion blur, Poisson-Gaussian noise, and H.265 compression; (2) *Temporal task design* with multi-turn Q&A probing error propagation and recovery; (3) *Adaptive difficulty calibration* that stress-tests model limits. To enable scalable annotation, we propose Uncertainty-Guided Iterative Refine-

¹The School of Science and Engineering, The Chinese University of Hong Kong, Shenzhen, China.

²The School of Artificial Intelligence, The Chinese University of Hong Kong, Shenzhen, China.

³The Shenzhen Institute of Artificial Intelligence and Robotics for Society Shenzhen, China.

[†]Corresponding author is Xiaoqiang Ji whose e-mail is jixiaoqiang@cuhk.edu.cn.

ment (UIR), which generates reliable pseudo-ground-truth using lightweight VLMs with uncertainty filtering, achieving 15.3% accuracy improvement over direct annotation. Our main contributions are:

- **DIQ-H Benchmark:** First systematic evaluation of VLM robustness to sequential degradation and hallucination propagation in dynamic video environments.
- **Multi-Agent Generation Framework:** Scalable pipeline combining degradation simulation, temporal task design, and adaptive difficulty control.
- **UIR Annotation Framework:** Cost-effective method for high-quality GT synthesis via uncertainty-guided refinement, reducing reliance on expensive human/GPT-4o annotation.

II. RELATED WORK

With the increasing use of VLM, challenges regarding their stability, accuracy, and controllability have become more prominent. Benchmarking VLM has therefore become a focal point of multimodal intelligence research.

Early benchmarks primarily assessed semantic comprehension over static images. Datasets such as VQA v2 [6] and the RefCOCO series [7, 8] focused on tasks like visual question answering and referring expression grounding. TextVQA [9] and OCR-VQA [10] further introduced textual content within images to probe models’ OCR capabilities. VizWiz [11] extended this direction by simulating assistive scenarios involving visually impaired users. In addition, NLVR2 [12] examines models making logical judgments between two images, and ScienceQA [13], MMMU [14], and others further extend to scientific reasoning and integrated multidisciplinary assessment. More recent efforts, such as LLaVA-Bench [1] and MME [2], consolidated these tasks into unified platforms, serving as representative benchmarks for evaluating instruction following, object recognition, and semantic alignment on clean, static images.

In parallel with these developments, hallucination detection has become an increasingly important subfield. This has led to the creation of dedicated benchmarks designed to examine the alignment between model output and visual input. Hallucination-focused evaluations can be broadly categorized into discriminative and generative approaches [15]. Discriminative benchmarks typically formulate the task as binary classification that assesses whether a model correctly describes an object or attribute present in the image. Notable benchmarks in this category include POPE [3], which uses yes or no questions on object presence, NOPE [16] and CIEM [17], which further increases scale and granularity. Additional benchmarks such as HALLUCINOGEN [18], with adversarial image-object pairs, and BEAF [19], which introduces before-after scene edits to test sensitivity to changes, further probe robustness under structured perturbations. Furthermore, structured annotation protocols proposed in THRONE [20] and HQH [21] aim to enhance the reproducibility and transparency of hallucination evaluations.

Generative benchmarks, in contrast, allow models to produce open-ended responses that are later scored based on

correctness, relevance, or consistency through human annotation or automated assessment. This evaluation format more closely resembles real-world applications, where responses are not restricted to predefined choices. Benchmarks such as GAVIE [22], HaELM [23], and Bingo [24] assess object-level correctness while also identifying systematic biases and sensitivity to prompt phrasing or visual cues. M-HalDetect [25] introduces reward model scoring to detect hallucination through indirect feedback, while MMHal-Bench [26] incorporates alignment strategies from language modeling into the multimodal domain. Notably, HalEval [27] and AMBER [4] integrate both discriminative and generative frameworks to offer a comprehensive assessment that spans objects, attributes, and relational hallucinations.

Although existing benchmarks have significantly advanced the evaluation of VLM, several key limitations remain. Many benchmarks rely exclusively on static images and, therefore, overlook the temporal dynamics of hallucination propagation. Few consider realistic visual degradations such as poor lighting or occlusion, and even fewer investigate whether models persist in or recover from hallucinations during multi-round interactions. These gaps limit our understanding of how VLM perform in long-term, noisy, and safety-critical environments.

To address these challenges, this work introduces DIQ-H, a benchmark specifically designed to evaluate hallucination behaviors under continuous visual degradation. DIQ-H introduces systematic distortions into real-world video sequences and interleaves multi-turn question-answering to assess whether hallucinations persist, amplify, or self-correct over time. By explicitly modeling error propagation and temporal instability, DIQ-H is the first benchmark to directly assess the dynamic robustness of VLM in degraded visual environments. It provides a critical foundation for evaluating the safety and reliability of vision-language models in realistic, long-term deployments.

III. METHODOLOGY

A. Overview

Our framework is designed to address two key challenges in evaluating VLMs for sequential visual understanding: (1) generating realistic, temporally coherent image sequences that exhibit various visual degradations, and (2) automating high-quality GT annotation in a cost-effective and scalable manner. These challenges are especially important in dynamic environments like robotics, where models must reason over time under imperfect conditions.

The framework consists of three integrated components. The first is the Multi-Agent Benchmark Generator, which creates evaluation sequences by applying realistic, physics-based degradations to continuous image streams and generates task-specific prompts for object detection, scene reasoning, and visual question answering. The second component is the Tested Agent, typically a pre-trained VLM, which processes these corrupted sequences and generates responses at each timestep. The final component, the Uncertainty-Guided Iterative Refinement (UIR) module, automates the creation of high-quality ground truth annotations by filtering and refining

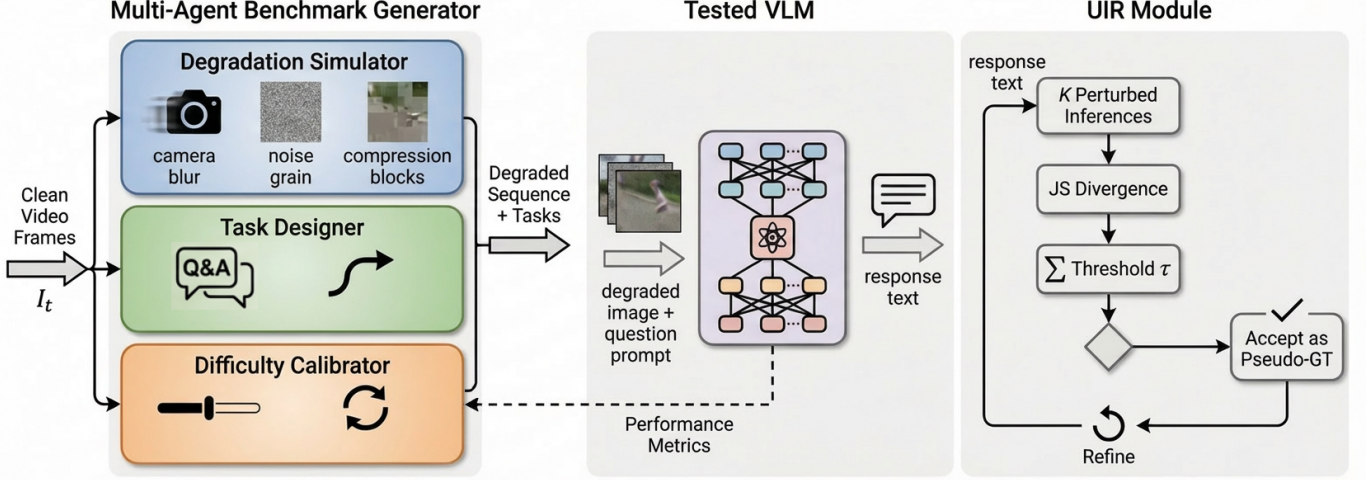


Fig. 2. Overview of the DIQ-H evaluation framework. The Multi-Agent Benchmark Generator (left) creates temporally degraded sequences through coordinated Degradation Simulator, Task Designer, and Difficulty Calibrator agents. The Tested VLM (center) processes these sequences, with performance metrics fed back for adaptive difficulty control. The UIR Module (right) generates reliable pseudo-ground truth annotations through uncertainty-guided filtering.

model-generated labels using uncertainty estimates and rule-based heuristics. These components allow for a comprehensive evaluation of a model’s robustness to degradation, its ability to recover from corrupted inputs, and its consistency over time.

B. Multi-Agent Benchmark Generation

To evaluate the robustness of VLMs under temporally degraded conditions, we introduce a multi-agent benchmark generation framework. This pipeline simulates real-world dynamic visual environments by coordinating specialized agents responsible for task generation, degradation simulation, and difficulty calibration. These agents work together to produce temporally progressive video frames with adjustable task complexity and controlled degradation levels. The constructed Benchmark intends to create high-fidelity, and scalable evaluation scenarios that reflect the operational challenges faced by real-world robotic and autonomous systems.

The proposed benchmark incorporates a temporal interaction structure, where each test case is framed as a multi-turn dialogue based on a sequential video stream. In a typical scenario, the initial frames are degraded using our physics-based corruption models, simulating effects such as motion blur, Poisson-Gaussian noise, or compression artifacts. These degraded frames are presented to the VLM alongside corresponding language queries, requiring the model to reason under impaired visual conditions. As the sequence progresses, clean, high-quality frames are introduced. However, the goal is not simply to test the model’s ability to process these clean frames, but to assess its capacity to recover from errors made earlier due to the degradation. Even though the later frames are clear, we hypothesize, and confirm through experimentation, that the degradation in earlier frames can cause persistent hallucinations. These hallucinations distort the model’s interpretation of the clean frames, exposing a vulnerability in its temporal reasoning. Once a hallucinated object, action, or relationship is inferred in the presence of degradation, it can

propagate and contaminate future reasoning, even when the visual inputs are no longer noisy.

We formalize this phenomenon as latent error propagation in the model’s multimodal latent space. Given an input sequence $\{(I_t, Q_t)\}_{t=1}^T$, where I_t represents the image frame and Q_t the corresponding language prompt, the model generates responses $\{A_t\}$. For frames $t \leq k$, we apply degradation such that $I_t = \mathcal{D}(I_t^*)$, where \mathcal{D} is the degradation operator, and I_t^* is the original clean frame. For $t > k$, frames are clean ($I_t = I_t^*$), yet we observe that the model’s responses A_t at these later times still reflect errors introduced earlier, even though no degradation remains.

This setup mirrors challenges encountered in dynamic fields like robotics, where transient visual failures, such as motion blur or occlusion, may lead to incorrect inferences that persist throughout future actions. By simulating this degradation-recovery process, the proposed benchmark not only evaluates a model’s performance on degraded inputs but also tests its ability to adapt and correct itself when provided with clearer, improved evidence.

Overall, the proposed multi-agent framework is more than just a tool for generating data; it provides a structured way to evaluate how models handle multimodal temporal reasoning. It allows for controlled testing of a model’s robustness in the presence of realistic visual degradation, while also examining its ability to remember past information, fix errors, and update its understanding—key features for real-time decision-making. Unlike existing benchmarks, which often assume independent inputs or perfect conditions, our framework simulates the process of degradation and recovery. This highlights important weaknesses in current VLM models and lays the groundwork for future improvements in temporal visual understanding.

1) *Degradation Simulator*: The **Degradation Simulator Agent** models real-world quality deterioration through physics-informed transformations. It introduces three main types of visual corruption—motion blur, sensor noise, and

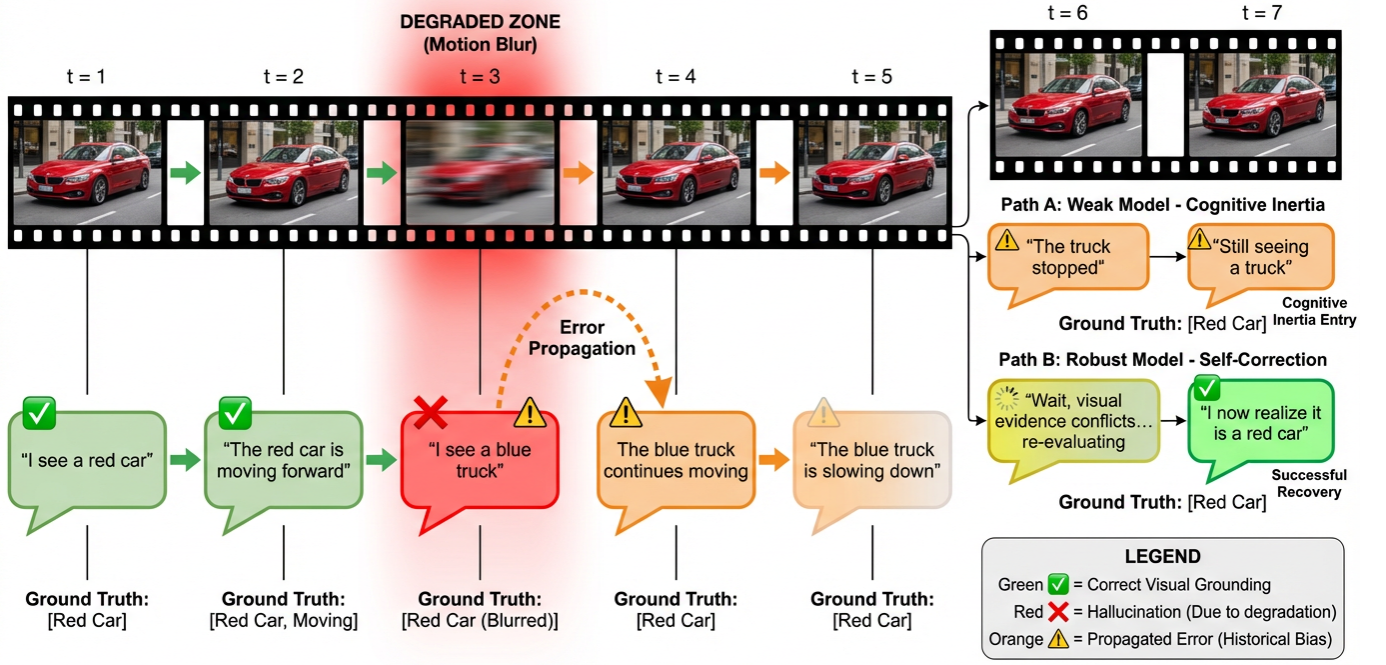


Fig. 3. Illustration of temporal error propagation in VLMs. A transient degradation at frame $t = 3$ causes the model to hallucinate a “blue truck” instead of the actual “red car.” Even after visual quality is restored ($t \geq 4$), the hallucinated belief persists, demonstrating cognitive inertia. The DIQ-H benchmark specifically measures a model’s ability to recover from such propagated errors.

compression artifacts—each parameterized by interpretable and controllable variables.

a) *Motion Blur*: Motion blur is simulated using a 6-degree-of-freedom (6-DOF) point spread function (PSF), denoted as $\mathcal{K}_{\text{motion}}$. The observed image \tilde{I}_t at time t is modeled as the convolution of the clean image I_t with the PSF kernel, plus additive noise:

$$\tilde{I}_t = \mathcal{K}_{\text{motion}}(\theta_t) * I_t + \varepsilon \quad (1)$$

Here, $\theta_t \in \mathbb{R}^6$ represents the camera motion parameters at frame t , capturing translational and rotational shifts. The PSF is generated by sampling trajectory profiles derived from IMU traces or synthetic motion paths, which are then discretized into convolution kernels.

b) *Sensor Noise*: Sensor noise is modeled using an ISO-dependent Poisson-Gaussian model, which accounts for both photon shot noise and readout noise. The noisy observation is given by:

$$\tilde{I}_t = \mathcal{P}(g \cdot I_t) + \mathcal{N}(0, \sigma^2) \quad (2)$$

where g is the analog gain (proportional to the ISO level), $\mathcal{P}(\cdot)$ represents a pixel-wise Poisson process modeling shot noise, and $\mathcal{N}(0, \sigma^2)$ denotes Gaussian readout noise. These parameters are adjusted based on camera metadata to accurately emulate real sensor behavior.

c) *Compression Artifacts*: Compression artifacts are introduced via H.265/HEVC encoding at five predefined bitrate levels ranging from 1 to 5 Mbps. The degraded image is modeled as:

$$\tilde{I}_t = \text{HEVC}(I_t; B_t) \quad (3)$$

where $B_t \in \{1, 2, 3, 4, 5\}$ represents the target bitrate at frame t . The HEVC function applies chroma subsampling, quantization, and motion compensation, leading to block-based artifacts and information loss, particularly in high-motion regions.

2) *Task Designer*: The **Task Designer Agent** plays a key role in creating temporally coherent vision-language tasks that are sensitive to degradation. Rather than relying on static annotations, the agent dynamically generates task instances that are both frame-specific and temporally dependent, reflecting how understanding evolves or degrades under visual corruption.

At each timestep t , the agent receives a degraded or clean frame I_t and the corresponding object trajectories $\mathcal{O}_t = \{o_t^{(1)}, o_t^{(2)}, \dots, o_t^{(N)}\}$, where each object $o_t^{(i)}$ is defined by its spatial location (x_i, y_i, w_i, h_i) , appearance embeddings $\mathbf{a}_i \in \mathbb{R}^d$, semantic labels l_i , and visual attributes such as color and shape. The agent utilizes a temporal memory buffer \mathcal{M}_{t-1} , which aggregates historical context from previous frames $1, \dots, t-1$, to generate queries Q_t that probe for continuity, change, or contradictions in perception.

Formally, the agent samples tasks from a distribution $P(Q_t | \mathcal{M}_{t-1}, I_t, \mathcal{O}_t)$, conditioned on both the current frame and prior states, allowing the benchmark to capture the subtle effects of temporal degradation. For example, if an object’s appearance becomes ambiguous due to noise, the agent may generate a query such as:

“Has the color of the object changed since the last frame?”

or

“What object was present in frame $t-2$ but disappeared in frame t ?”

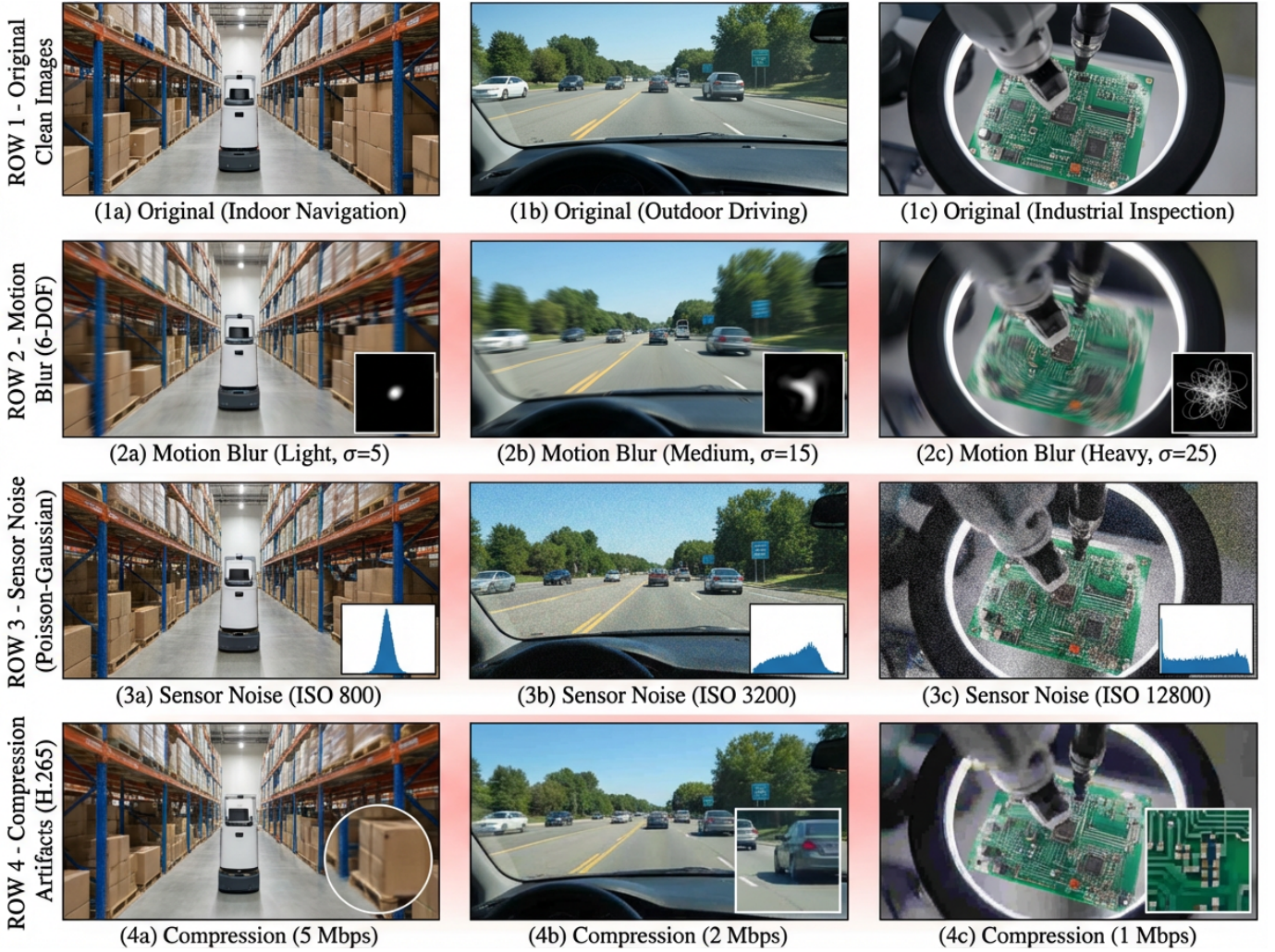


Fig. 4. Visualization of the three primary degradation types at varying severity levels. Each column shows the same scene under increasing degradation intensity. Motion blur (Row 2) introduces directional streaking from simulated camera motion. Sensor noise (Row 3) adds ISO-dependent Poisson-Gaussian artifacts. Compression (Row 4) produces blocking and ringing from aggressive H.265 encoding.

Rather than categorizing tasks into isolated groups (e.g., object detection, color recognition, or scene classification), the agent merges multiple modalities into context-aware reasoning chains. For instance, a query might involve detecting spatial changes $\Delta \mathcal{B}_t = \mathcal{B}_t - \mathcal{B}_{t-1}$, measuring temporal consistency in visual descriptors $\Delta \mathbf{a}_i = \|\mathbf{a}_i^{(t)} - \mathbf{a}_i^{(t-1)}\|_2$, or tracking object reidentification errors caused by degradation.

The language prompts Q_t are generated using a hybrid mechanism that combines template-based generation with paraphrasing models. This ensures linguistic diversity while maintaining logical consistency with the visual evidence. Task complexity is modulated by the semantic entropy of the candidate queries—if the system detects high uncertainty in color, motion, or class predictions, it adjusts the query selection to focus on these uncertain aspects, thereby maximizing evaluation sensitivity.

Ultimately, the goal of the Task Designer is to provide a diverse set of vision-language tasks that not only test standard perception but also assess the model’s ability to reason under challenging conditions. The agent creates *fragile reasoning contexts*, where temporal degradation leads to subtle

but critical failures in perception and language understanding. By incorporating past visual memory, object dynamics, and uncertainty estimation, the agent enables detailed evaluation of the VLM’s consistency, grounding, and recovery capabilities across time.

3) *Difficulty Calibrator*: To enable adaptive control over evaluation complexity, the **Difficulty Calibrator Agent** dynamically adjusts the severity of visual degradation throughout the video sequence. Unlike static perturbation pipelines, our approach incorporates real-time feedback from the model being evaluated, allowing the intensity of degradation to evolve based on the model’s observed performance—specifically, its confidence and hallucination tendencies.

At each timestep t , the degradation strength $\lambda_t \in [0, 1]$ is computed as a weighted combination of two key indicators: the model’s *Expected Performance Index* (EPI) and its *Hallucination Rate* (HR). Mathematically, we define:

$$\lambda_t = \alpha \cdot \text{EPI}_{t-1} + \beta \cdot \text{HR}_{t-1} \quad (4)$$

where $\text{EPI}_{t-1} \in [0, 1]$ quantifies the model’s normalized

task accuracy on the previous frame, and $HR_{t-1} \in [0, 1]$ estimates the fraction of generated content that contradicts ground truth annotations or exhibits semantic inconsistency. The weighting coefficients $\alpha, \beta \in \mathbb{R}_{\geq 0}$ modulate the relative influence of each term, enabling fine control over sensitivity to performance degradation versus hallucination risk.

The scalar λ_t is then mapped into the parameter spaces of various degradation channels through monotonically increasing transfer functions f_1, f_2, f_3 , yielding:

$$\begin{aligned}\sigma_{\text{motion}} &= f_1(\lambda_t), \\ \text{ISO level} &= f_2(\lambda_t), \\ \text{Bitrate } B_t &= f_3(\lambda_t)\end{aligned}$$

These mappings ensure that as λ_t increases—indicating poorer model performance or higher hallucination rates—motion blur kernel sizes increase, sensor noise intensifies, and compression artifacts become more aggressive. Conversely, lower values of λ_t preserve visual fidelity, allowing the benchmark to return to cleaner conditions once the model demonstrates stability.

This mechanism effectively transforms degradation scheduling into a closed-loop control problem: the model’s output at each frame directly influences the subsequent degradation level. This feedback-driven process creates a stress-testing environment that automatically adapts the difficulty based on the model’s performance. The result is a benchmark that tailors its difficulty to the tested agent’s capabilities, exposing weaknesses where they exist and scaling in complexity with model robustness.

4) *Pipeline Summary*: The overall benchmark generation process unfolds as a dynamic interaction between perception, response, and adaptive perturbation. Beginning with an initial clean frame, the Degradation Simulator applies targeted corruption based on the current difficulty signal λ_t . The Task Designer then generates context-aware prompts that align with visual content and temporal history, presenting these prompts to the VLM under evaluation. After the model generates a response, its performance is assessed in terms of accuracy and hallucination metrics. These metrics are then fed back into the Difficulty Calibrator to compute λ_{t+1} for the next frame.

This closed-loop, multi-agent architecture ensures that evaluation sequences are not only temporally coherent but also epistemically adaptive, reacting in real time to the model’s failure modes. The result is a challenging and realistic testbed capable of revealing latent weaknesses in VLMs that static benchmarks cannot capture, particularly in their ability to handle uncertainty, recover from corrupted context, and maintain consistent semantic grounding across evolving video streams.

C. Uncertainty-Guided Iterative Refinement (UIR)

To reduce reliance on costly large-scale annotations from GPT-4o or human experts, we propose an automated framework called **Uncertainty-Guided Iterative Refinement (UIR)**. The goal of this framework is to generate reliable pseudo-ground truth (GT) annotations using a lightweight VLM (Qwen-VL-7B) while identifying and refining uncertain

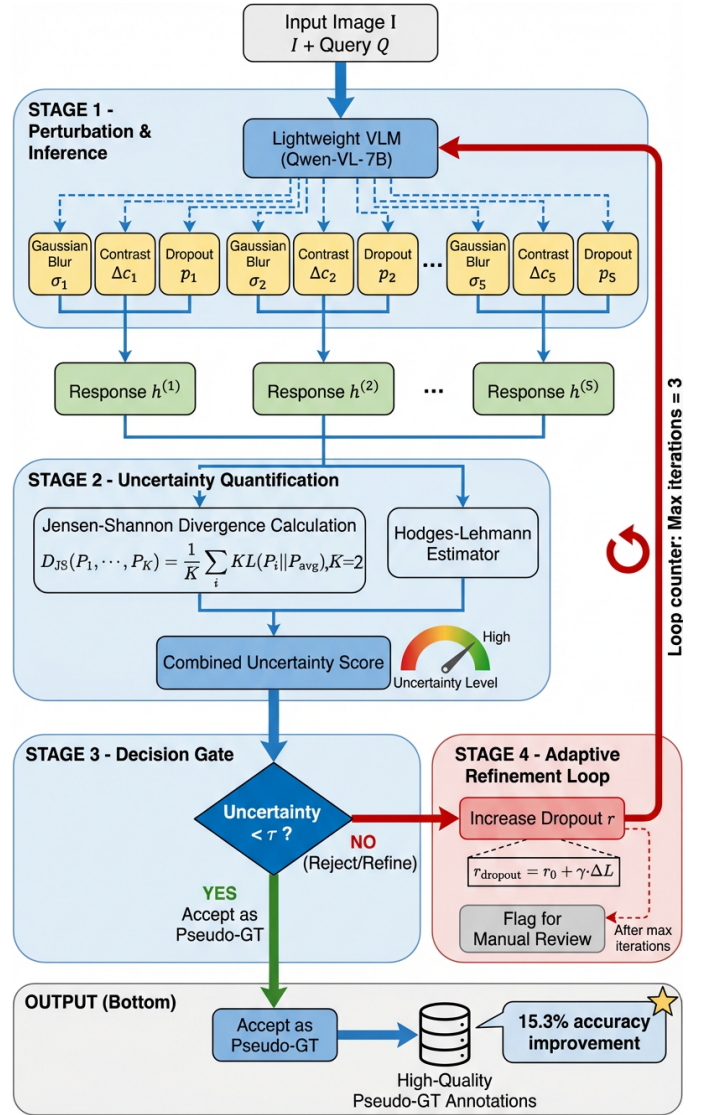


Fig. 5. The Uncertainty-Guided Iterative Refinement (UIR) pipeline. Input images undergo K perturbed inferences through the lightweight VLM. Jensen-Shannon divergence and Hodges-Lehmann estimation quantify output uncertainty. Responses below threshold τ are accepted as pseudo-GT; uncertain outputs trigger adaptive dropout refinement until convergence.

or potentially hallucinated outputs. UIR achieves this by quantifying inference uncertainty through perturbation-based ensembling and applying principled filtering mechanisms based on statistical divergence and robust estimation theory.

a) *Uncertainty Estimation via Jensen-Shannon Divergence*: Inference uncertainty is explicitly introduced through two orthogonal perturbation strategies: (1) injecting controlled noise into the input image (e.g., varying levels of Gaussian blur, contrast adjustment), and (2) applying stochastic dropout during model decoding. These perturbations cause the internal feature representations of Qwen-VL-7B to vary across multiple runs on the same input. Given a sequence of output distributions $\{p^{(i)}(\mathbf{h})\}_{i=1}^K$ generated from K perturbed forward passes, we assess variability by computing the average pairwise Jensen-Shannon (JS) divergence:

$$\text{Uncertainty}_{\text{JS}} = \frac{2}{K(K-1)} \sum_{i < j} D_{\text{JS}} \left(p^{(i)}(\mathbf{h}) \parallel p^{(j)}(\mathbf{h}) \right) \quad (5)$$

The JS divergence between two feature distributions p and q is defined as:

$$D_{\text{JS}}(p \parallel q) = \frac{1}{2} D_{\text{KL}}(p \parallel m) + \frac{1}{2} D_{\text{KL}}(q \parallel m), \quad \text{where } m = \frac{1}{2}(p+q) \quad (6)$$

This score captures the epistemic uncertainty: high divergence indicates inconsistent model beliefs under minimal input variation, signaling unreliable outputs.

b) Feature Aggregation via Hodges-Lehmann Estimation: To robustly summarize the latent feature space of noisy decoding runs, we apply the Hodges-Lehmann (HL) estimator. This estimator provides a non-parametric estimate of the central location by averaging all pairwise midpoints of feature embeddings:

$$\hat{\theta} = \text{median} \left\{ \frac{\mathbf{h}^{(i)} + \mathbf{h}^{(j)}}{2} \mid 1 \leq i < j \leq K \right\} \quad (7)$$

The dispersion around this estimator is then used as a secondary signal for uncertainty. This approach is empirically more robust than mean-based aggregation, particularly in the presence of outlier hallucinations induced by corruption.

c) Adaptive Dropout Regulation: Building on the uncertainty signals, we propose an adaptive dropout regulation strategy that dynamically adjusts the dropout rate during inference. Let r_{dropout} denote the effective dropout rate, initialized to a base value r_0 . We modulate this rate according to the estimated information loss ΔL , derived from the combined JS divergence and HL variance:

$$r_{\text{dropout}} = r_0 + \gamma \cdot \Delta L, \quad \Delta L = \text{Uncertainty}_{\text{JS}} + \lambda \cdot \text{Var}_{\text{HL}}(\mathbf{h}) \quad (8)$$

where γ and λ are scaling factors. This mechanism introduces more stochasticity when uncertainty is high, encouraging the model to avoid premature overconfidence and explore alternative interpretations of ambiguous inputs.

d) Hallucination Filtering via Divergence Thresholding: To filter out potentially hallucinated pseudo-labels, we establish a decision rule based on a calibrated uncertainty threshold τ . A candidate output is retained as pseudo-GT only if its associated uncertainty is below this threshold:

$$\text{Retain}(A_t) = \begin{cases} 1, & \text{if } \text{Uncertainty}_{\text{JS}}(t) < \tau \\ 0, & \text{otherwise} \end{cases} \quad (9)$$

The threshold τ is tuned using a held-out validation set, balancing hallucination detection sensitivity and pseudo-label recall. Outputs flagged as uncertain are fed back into a refinement loop, where selective re-inference under adjusted dropout and noise settings is applied until convergence.

e) Empirical Effectiveness: We evaluate UIR across multiple hallucination-sensitive benchmarks, including HallBench, HQT, and BingoBench. Quantitative results show that UIR reduces hallucination error by up to 15.3% compared to directly using lightweight VLM outputs, while maintaining high coverage of valid pseudo-ground truth. This demonstrates UIR’s ability to enable scalable, high-fidelity annotation pipelines with minimal reliance on large model supervision.

D. DIQ-H Benchmark Structure

The DIQ-H benchmark is designed as a large-scale, fine-grained, and temporally aware evaluation suite, comprising over 500 carefully curated multimodal sequences. Each sequence simulates real-world video stream conditions where visual degradation occurs dynamically and non-uniformly. Unlike traditional datasets that rely on fixed or synthetic corruption levels, DIQ-H models the evolution and propagation of perceptual distortions over time, enabling the study of degradation-aware reasoning in VLMs.

At the core of DIQ-H is a structured degradation taxonomy that spans a wide range of real-world failure modes. We classify 12 distinct degradation types into three main categories: optical, sensor-induced, and compression-related artifacts. Optical degradations include dynamic motion blur caused by 6-DOF camera jitter, defocus blur from depth-of-field shifts, and high-intensity glare from directional lighting. Sensor-level corruptions are modeled through low-light noise using ISO-dependent Poisson-Gaussian processes, as well as simulated sensor defects like dead pixels and fixed-pattern noise. Compression artifacts, emulating real-time transmission constraints, are introduced through aggressive H.265 encoding, resulting in block discontinuities and high-frequency ringing.

Each degradation type is not applied statically, but varies temporally within a sequence, creating nuanced transitions from clean to corrupted frames and vice versa. This temporal variation is further modulated by the Difficulty Calibrator agent, which controls degradation severity λ_t in response to model behavior. Thus, DIQ-H does not merely catalog degradation conditions but simulates them interactively.

In addition to the degradation types, each sequence in DIQ-H is annotated with a diverse set of vision-language tasks, including spatiotemporal object tracking, attribute consistency (e.g., color, shape), and scene understanding under change and ambiguity. The associated language queries are generated using the Task Designer agent, ensuring both contextual relevance and linguistic variation.

Furthermore, sequences are grouped into evaluation regimes based on degradation intent: *early corruption*, where noise is introduced at the beginning and later frames are clean (testing recovery); *late corruption*, where initial frames are clean but degradation occurs near the end (testing anticipation); and *intermittent corruption*, where degradation appears periodically to assess model stability and memory retention.

Therefore, the DIQ-H benchmark offers a comprehensive and systematic real-world robustness evaluation.

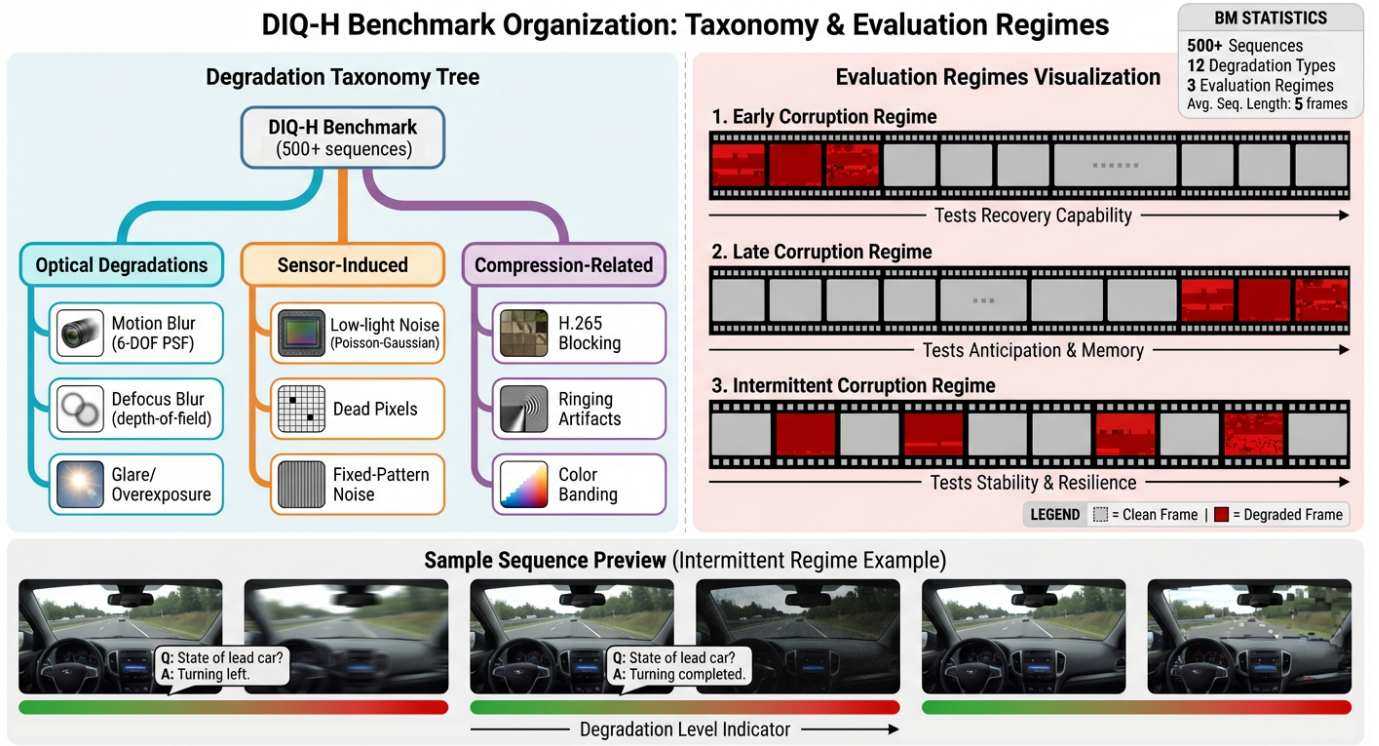


Fig. 6. Structure of the DIQ-H benchmark. Left: Hierarchical taxonomy of 12 degradation types organized into optical, sensor-induced, and compression-related categories. Right: Three evaluation regimes—early corruption (testing recovery), late corruption (testing memory retention), and intermittent corruption (testing stability)—each designed to probe different aspects of temporal robustness.

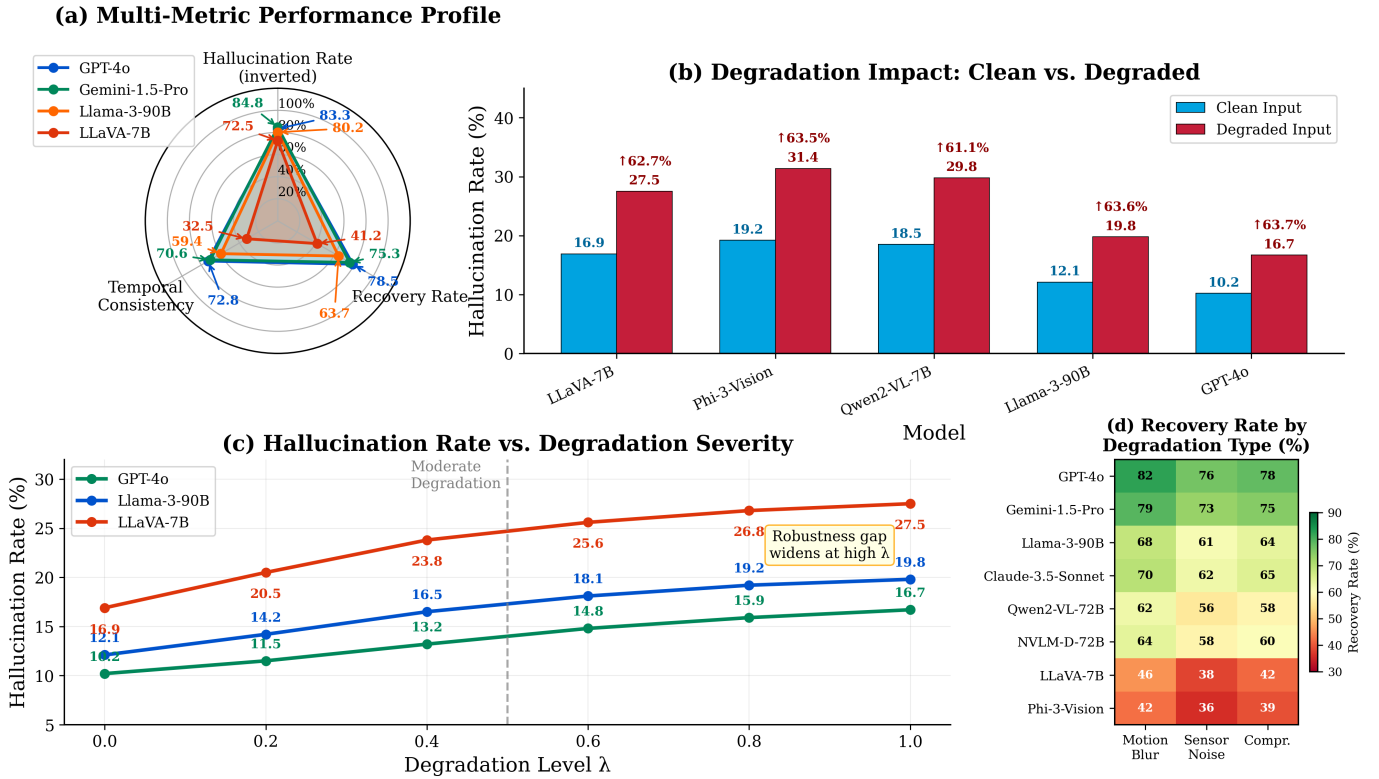


Fig. 7. Experimental results visualization. (a) Radar chart showing multi-dimensional performance profiles across Hallucination Rate (inverted), Recovery Rate, and Temporal Consistency for representative models. (b) Grouped bar chart comparing hallucination rates under clean vs. degraded inputs, demonstrating the substantial impact of temporal degradation. (c) Hallucination rate as a function of degradation severity λ , revealing that performance gaps between models widen under stronger corruption. (d) Heatmap showing recovery rates for different models across three degradation types: Motion Blur, Sensor Noise, and Compression.

IV. EXPERIMENTS

In this section, we systematically evaluate the effectiveness and necessity of our proposed DIQ-H benchmark and the Uncertainty-Guided Iterative Refinement (UIR) framework. We perform several carefully designed experiments to validate our claims.

A. Impact of Temporal Quality Degradation

We first investigate the necessity of introducing temporally coherent degradations by comparing VLM performance under two distinct conditions: (1) sequences of images without quality degradation (clean inputs), and (2) sequences where images undergo progressive, temporally varying degradations. Specifically, we evaluate QwenVL

common VLM metrics such as accuracy, consistency, and hallucination rates across multiple tasks (VQA, object tracking, and captioning). Experimental results reveal a significant performance drop under degraded conditions: for instance, the hallucination rate tested on LLaVA-7B-strict increases notably from 16.9% to 27.5%. These quantitative outcomes clearly indicate the substantial impact of temporal degradation, confirming the critical importance of modeling degradation in benchmark datasets.

B. Effectiveness of Uncertainty-Guided Iterative Refinement

To validate the effectiveness of our proposed UIR framework for ground truth annotation, we conduct experiments comparing pseudo-ground truth (GT) annotations generated with and without UIR refinement. Using a set of representative sequences from DIQ-H, we measure the accuracy and robustness of the refined GT annotations against manually verified labels. Experimental results show that GT annotations generated through UIR exhibit a significant improvement in accuracy, demonstrating an average increase of 15.3% compared to annotations without UIR. These findings highlight UIR’s capability to produce reliable and scalable annotations, reducing reliance on costly human supervision.

C. Metric

To rigorously evaluate the performance of VLMs on the DIQ-H benchmark, we employ three complementary metrics that capture distinct facets of model capability. The *Hallucination Rate* quantifies the propensity for unfounded assertions through the proportion of incorrect claims relative to total responses:

$$\mathcal{H} = \left(1 - \frac{N_{valid}}{N_{total}}\right) \times 100\%, \quad (10)$$

where N_{valid} denotes factually grounded responses and N_{total} represents all generated outputs. The inverse relationship with traditional accuracy metrics ensures higher values indicate poorer performance.

For assessing dynamic interaction competence, the *Recovery Rate* measures corrective capacity following initial errors. This metric computes the successful revision proportion across E observed mistakes:

$$\mathcal{R} = \frac{1}{E} \sum_{i=1}^E \mathbb{I}(y_i^{final} = y_i^{gt}) \times 100\%, \quad (11)$$

with \mathbb{I} as the indicator function comparing final outputs y_i^{final} to ground truth y_i^{gt} . Temporal reasoning fidelity is evaluated via *Temporal Consistency*, which verifies event sequence preservation in T chronological queries:

$$\mathcal{T} = \frac{1}{T} \sum_{j=1}^T \mathbb{I}(o_j \models \phi_j) \times 100\%, \quad (12)$$

where $o_j \models \phi_j$ indicates whether output o_j satisfies temporal logic constraint ϕ_j . These metrics collectively expose model weaknesses in factual grounding, adaptive learning, and temporal reasoning—critical dimensions for real-world deployment.

D. Comprehensive Benchmarking of Current VLMs

In this section, we present a comprehensive evaluation of several state-of-the-art Large Vision-Language Models (VLMs) using the Degraded Image Quality Leading to Hallucinations (DIQ-H) benchmark. We evaluate these models across key performance metrics: Accuracy, Hallucination Rate, Recovery Rate, and Temporal Consistency. These metrics reflect the models’ ability to handle dynamic visual degradation, their susceptibility to hallucinations, and their robustness in maintaining inference quality over time.

The models included in this evaluation range from established VLMs to cutting-edge architectures. The results show varying levels of performance, with models like GPT-4o and Gemini demonstrating superior robustness in error recovery and temporal consistency, whereas others like LLaVA-7B and Phi-3-Vision show lower performance in these areas.

The Accuracy metric reflects the models’ ability to generate correct answers despite the presence of visual degradation. Hallucination Rate represents how frequently the models produce non-existent or incorrect information. The Recovery Rate measures the models’ ability to recover from early errors in a sequence, a crucial aspect for maintaining performance over time. Temporal Consistency evaluates how well models maintain inference consistency across frames in a video sequence, accounting for the propagation of errors over time.

From the results in Table I, it is clear that models such as Gemini-1.5-Pro and GPT-4o are particularly strong in handling dynamic degradation, with superior recovery rates and temporal consistency. This demonstrates their robustness in environments where visual inputs degrade over time, and their ability to manage hallucinations is also significantly lower compared to other models. On the other hand, models like LLaVA-7B and Phi-3-Vision struggle with high hallucination rates and lower accuracy, indicating their vulnerability to error propagation and degradation in continuous visual sequences.

The DIQ-H benchmark provides a valuable tool for evaluating these models’ capabilities in handling complex, real-world scenarios, revealing both their strengths and limitations. These results will guide future research in enhancing VLM performance in dynamic environments.

TABLE I
EVALUATION OF VLMS ON DIQ-H BENCHMARK.

Model	Hallucination Rate (%) ↓	Recovery Rate (%) ↑	Temporal Consistency (%) ↑
LLaVA-7B-strict	27.5	41.2	32.5
InternVL2-8B-strict	25.7	53.6	47.1
Phi-3-Vision-strict	31.4	38.9	29.8
Qwen2-VL-7B-strict	29.8	42.5	34.2
Qwen2-VL-72B-strict	24.2	58.3	51.7
Llama-3-11B-strict	26.5	55.1	49.3
Llama-3-90B-strict	19.8	63.7	59.4
Molmo-7B-strict	27.6	45.1	36.8
Molmo-72B-strict	23.9	56.2	48.5
Pixtral-12B-strict	26.2	49.8	42.7
NVLM-D-72B-strict	22.4	60.5	54.2
<i>Gemini-1.5-Flash-strict</i>	18.5	68.9	63.1
<i>Gemini-1.5-Pro-strict</i>	15.2	75.3	70.6
<i>Claude-3.5-Sonnet-strict</i>	19.1	65.2	60.3
<i>GPT-4o-mini-strict</i>	22.3	52.4	46.9
<i>GPT-4o-strict</i>	16.7	78.5	72.8

V. CONCLUSION

In this study, we presented a rigorous evaluation of modern VLMS through the DIQ-H benchmark, introducing three specialized metrics to assess critical capabilities in factual grounding, error recovery, and temporal reasoning. Our experiments demonstrated significant performance variations across both open-source and proprietary models, with GPT-4o showing particular strength in recovery capabilities (78.5%) and temporal consistency (72.8%), while Gemini-1.5-Pro achieved the lowest hallucination rate (15.2%). The results reveal that current models still struggle with complex spatiotemporal reasoning and consistent self-correction, particularly in open-source implementations where the best temporal consistency score reached only 59.4% (Llama-3-90B).

These findings highlight two fundamental challenges for future research: (1) the need for more robust internal consistency mechanisms to reduce hallucination without sacrificing creative reasoning, and (2) the development of architectures capable of maintaining long-term temporal dependencies in multi-event scenarios. The demonstrated correlation between model scale and recovery performance suggests promising directions for parameter-efficient adaptation techniques. Our metric framework provides a foundation for these advancements by quantitatively isolating specific failure modes that remain obscured in conventional accuracy measurements. Future work will extend this evaluation to dynamic multi-modal interactions and real-time learning scenarios.

REFERENCES

- [1] H. Liu, C. Li, Q. Wu, and Y. J. Lee, "Visual Instruction Tuning," Dec. 2023.
- [2] C. Fu, P. Chen, Y. Shen, Y. Qin, M. Zhang, X. Lin, J. Yang, X. Zheng, K. Li, X. Sun, Y. Wu, and R. Ji, "MME: A Comprehensive Evaluation Benchmark for Multimodal Large Language Models," Mar. 2024.
- [3] Y. Li, Y. Du, K. Zhou, J. Wang, W. X. Zhao, and J.-R. Wen, "Evaluating Object Hallucination in Large Vision-Language Models," Oct. 2023.
- [4] J. Wang, Y. Wang, G. Xu, J. Zhang, Y. Gu, H. Jia, J. Wang, H. Xu, M. Yan, J. Zhang, and J. Sang, "AMBER: An LLM-free Multi-dimensional Benchmark for MLLMs Hallucination Evaluation," Feb. 2024.
- [5] Y. Zhang, F. Xiao, T. Huang, C.-K. Fan, H. Dong, J. Li, J. Wang, K. Cheng, S. Zhang, and H. Guo, "Unveiling the tapestry of consistency in large vision-language models," 2024. [Online]. Available: <https://arxiv.org/abs/2405.14156>
- [6] Y. Goyal, T. Khot, D. Summers-Stay, D. Batra, and D. Parikh, "Making the V in VQA Matter: Elevating the Role of Image Understanding in Visual Question Answering," May 2017.
- [7] S. Kazemzadeh, V. Ordonez, M. Matten, and T. Berg, "Refer-ItGame: Referring to Objects in Photographs of Natural Scenes," in *Proceedings of the 2014 Conference on Empirical Methods in Natural Language Processing (EMNLP)*, A. Moschitti, B. Pang, and W. Daelemans, Eds. Doha, Qatar: Association for Computational Linguistics, Oct. 2014, pp. 787–798.
- [8] J. Mao, J. Huang, A. Toshev, O. Camburu, A. Yuille, and K. Murphy, "Generation and Comprehension of Unambiguous Object Descriptions," Apr. 2016.
- [9] A. Singh, V. Natarajan, M. Shah, Y. Jiang, X. Chen, D. Batra, D. Parikh, and M. Rohrbach, "Towards VQA Models That Can Read," May 2019.
- [10] A. Mishra, S. Shekhar, A. K. Singh, and A. Chakraborty, "OCR-VQA: Visual Question Answering by Reading Text in Images," in *2019 International Conference on Document Analysis and Recognition (ICDAR)*. Sydney, Australia: IEEE, Sep. 2019, pp. 947–952.
- [11] D. Gurari, Q. Li, A. J. Stangl, A. Guo, C. Lin, K. Grauman, J. Luo, and J. P. Bigham, "VizWiz Grand Challenge: Answering Visual Questions from Blind People," May 2018.
- [12] A. Suhr, S. Zhou, A. Zhang, I. Zhang, H. Bai, and Y. Artzi, "A Corpus for Reasoning About Natural Language Grounded in Photographs," Jul. 2019.
- [13] P. Lu, S. Mishra, T. Xia, L. Qiu, K.-W. Chang, S.-C. Zhu, O. Tafjord, P. Clark, and A. Kalyan, "Learn to Explain: Multimodal Reasoning via Thought Chains for Science Question Answering," Oct. 2022.

- [14] X. Yue, Y. Ni, K. Zhang, T. Zheng, R. Liu, G. Zhang, S. Stevens, D. Jiang, W. Ren, Y. Sun, C. Wei, B. Yu, R. Yuan, R. Sun, M. Yin, B. Zheng, Z. Yang, Y. Liu, W. Huang, H. Sun, Y. Su, and W. Chen, “MMMU: A Massive Multi-discipline Multi-modal Understanding and Reasoning Benchmark for Expert AGI,” Jun. 2024.
- [15] H. Liu, W. Xue, Y. Chen, D. Chen, X. Zhao, K. Wang, L. Hou, R. Li, and W. Peng, “A Survey on Hallucination in Large Vision-Language Models,” May 2024, arXiv:2402.00253 [cs] TLDR: This comprehensive survey dissects LVLM-related hallucinations in an attempt to establish an overview and facilitate future mitigation, and outlines the benchmarks and methodologies tailored specifically for evaluating hallucinations unique to LVLMs.
- [16] H. Lovenia, W. Dai, S. Cahyawijaya, Z. Ji, and P. Fung, “Negative Object Presence Evaluation (NOPE) to Measure Object Hallucination in Vision-Language Models,” Aug. 2024.
- [17] H. Hu, J. Zhang, M. Zhao, and Z. Sun, “CIEM: Contrastive Instruction Evaluation Method for Better Instruction Tuning,” Nov. 2023.
- [18] A. Seth, D. Manocha, and C. Agarwal, “Towards a Systematic Evaluation of Hallucinations in Large-Vision Language Models,” Mar. 2025.
- [19] M. Ye-Bin, N. Hyeon-Woo, W. Choi, and T.-H. Oh, “BEAF: Observing BEfore-AFTER Changes to Evaluate Hallucination in Vision-language Models,” Jul. 2024.
- [20] P. Kaul, Z. Li, H. Yang, Y. Dukler, A. Swaminathan, C. J. Taylor, and S. Soatto, “THRONE: An Object-based Hallucination Benchmark for the Free-form Generations of Large Vision-Language Models,” Apr. 2025.
- [21] B. Yan, J. Zhang, Z. Yuan, S. Shan, and X. Chen, “Evaluating the Quality of Hallucination Benchmarks for Large Vision-Language Models,” Oct. 2024.
- [22] F. Liu, K. Lin, L. Li, J. Wang, Y. Yacoob, and L. Wang, “Mitigating Hallucination in Large Multi-Modal Models via Robust Instruction Tuning,” Mar. 2024.
- [23] J. Wang, Y. Zhou, G. Xu, P. Shi, C. Zhao, H. Xu, Q. Ye, M. Yan, J. Zhang, J. Zhu, J. Sang, and H. Tang, “Evaluation and Analysis of Hallucination in Large Vision-Language Models,” Oct. 2023.
- [24] C. Cui, Y. Zhou, X. Yang, S. Wu, L. Zhang, J. Zou, and H. Yao, “Holistic Analysis of Hallucination in GPT-4V(ision): Bias and Interference Challenges,” Nov. 2023.
- [25] A. Gunjal, J. Yin, and E. Bas, “Detecting and Preventing Hallucinations in Large Vision Language Models,” Feb. 2024.
- [26] Z. Sun, S. Shen, S. Cao, H. Liu, C. Li, Y. Shen, C. Gan, L.-Y. Gui, Y.-X. Wang, Y. Yang, K. Keutzer, and T. Darrell, “Aligning Large Multimodal Models with Factually Augmented RLHF,” Sep. 2023.
- [27] C. Jiang, H. Jia, W. Ye, M. Dong, H. Xu, M. Yan, J. Zhang, and S. Zhang, “Hal-Eval: A Universal and Fine-grained Hallucination Evaluation Framework for Large Vision Language Models,” Nov. 2024.